Cell Host & Microbe
Article

Massive Secretion by T Cells Is Caused by HIV Nef in Infected Cells and by Nef Transfer to Bystander Cells

Claudia Muratori,[1,2] Lucas E. Cavallin,[1] Kirsten Krätzel,[5] Antonella Tinari,[3] Angelo De Milito,[4] Stefano Fais,[4] Paola D'Aloja,[2] Maurizio Federico,[2] Vincenzo Vullo,[6] Alla Fomina,[7] Enrique A. Mesri,[1] Fabiana Superti,[3] and Andreas S. Baur[1,5,*]
[1]Department of Microbiology and Immunology, University of Miami, Miller School of Medicine, Miami, FL 33136, USA
[2]National AIDS Centre
[3]Department of Technology and Health
[4]Department of Therapeutic Research and Medicines Evaluation, Unit of Antitumor Drugs
Istituto Superiore di Sanità, 00161 Rome, Italy
[5]Department of Dermatology, University of Erlangen/Nürnberg, 91054 Erlangen, Germany
[6]Department of Infectious and Tropical Diseases, La Sapienza University, Rome, Italy
[7]Department of Physiology and Membrane Biology, University of California, Davis, CA 95616, USA
*Correspondence: andreas.baur@uk-erlangen.de
DOI 10.1016/j.chom.2009.06.009

SUMMARY

The HIV Nef protein mediates endocytosis of surface receptors that correlates with disease progression, but the link between this Nef function and HIV pathogenesis is not clear. Here, we report that Nef-mediated activation of membrane trafficking is bidirectional, connecting endocytosis with exocytosis as occurs in activated T cells. Nef expression induced an extensive secretory activity in infected and, surprisingly, also in noninfected T cells, leading to the massive release of microvesicle clusters, a phenotype observed in vitro and in 36%–87% of primary CD4 T cells from HIV-infected individuals. Consistent with exocytosis in noninfected cells, Nef is transferred to bystander cells upon cell-to-cell contact and subsequently induces secretion in an Erk1/2-dependent manner. Thus, HIV Nef alters membrane dynamics, mimicking those of activated T cells and causing a transfer of infected cell signaling (TOS) to bystander cells. This mechanism may help explain the detrimental effect on bystander cells seen in HIV infection.

INTRODUCTION

Rapid progression of HIV infection in humans and animal models is closely linked to the function of the viral Nef protein (Deacon et al., 1995; Hanna et al., 1998; Kestler et al., 1991). In the presence of Nef, viral loads of up to 10^7 particles/ml are measured, whereas HIV is barely detectable in individuals infected with a Nef-negative mutant virus (Birch et al., 2001; Learmont et al., 1999; Saag et al., 1996). The molecular mechanism(s) by which Nef increases the viral load is (are) not understood; however, the protein seems to activate T cell signaling pathways that support this function by different means, including the promotion of particle release, viral infectivity, receptor downmodulation, and antiapoptotic signaling (Fackler and Baur, 2002; Wei et al., 2003).

There is evidence, however, that Nef functions other than those increasing viral load contribute to HIV pathogenesis. First, high viral loads may not necessarily cause immunodeficiency, as demonstrated for SIV-infected sooty mangabeys (Silvestri et al., 2003). Second, Nef-transgenic mice develop AIDS-like symptoms in the absence of viral replication (Hanna et al., 1998; Lindemann et al., 1994). Third, it has been suggested that Nef's ability to downregulate CD4 rather than its replication-promoting functions correlates with T cell depletion and pathogenesis (Hanna et al., 2006; Iafrate et al., 2000; Stoddart et al., 2003).

The downregulation of CD4 and MHCI was the first function ascribed to Nef and has been investigated thoroughly ever since (Garcia and Miller, 1991; Lama, 2003; Le Gall et al., 1998; Piguet et al., 1999). It is assumed that these receptors are transported into lysosomes for accelerated degradation (Aiken et al., 1994; Craig et al., 1998; Greenberg et al., 1997; Piguet et al., 1998; Rhee and Marsh, 1994). In recent years, numerous more receptors were found to be downregulated, including CD28 (Swigut et al., 2001), CD3 (only SIV) (Schaefer et al., 2000), CD80, CD86 (Chaudhry et al., 2005), CCR5 (Michel et al., 2005), and CD8 (Stove et al., 2005), whereas the invariant chain CD74 was upregulated (Stumptner-Cuvelette et al., 2001). The reason why so many receptors are downregulated is not known.

Increased receptor endocytosis in T cells is also a consequence of T cell receptor (TCR) activation (Geisler, 2004). In addition, the same stimulus activates exocytosis and secretion of different cytokines (Jolly and Sattentau, 2007). Therefore, in activated cells, both processes are tightly coordinated and mediated by an activation of bidirectional membrane trafficking (Gundelfinger et al., 2003). During this membrane transformation, larger endocytic compartments develop, like multivesicular bodies (MVBs) or secretory lysosomes, and different forms of vesicles are secreted, including exosomes (Fomina et al., 2003) and shedding microvesicles (Cocucci et al., 2009). These smaller vesicles contain a number of different surface molecules, including MHC complexes, death ligands (FasL, TRAIL), and

matrix metalloproteases (Cocucci et al., 2009; Théry et al., 2002). While their overall function is under debate, in vitro experiments suggest a role in priming CD8 T cells, exchange of membrane proteins (Théry et al., 2002), and induction of apoptosis (Andreola et al., 2002; Bossi and Griffiths, 1999; Martínez-Lorenzo et al., 1999; Monleón et al., 2001).

By employing a Nef-inducible system in combination with live video and electron microscopy (EM), we found that Nef induces bidirectional membrane trafficking identical to that in activated T cells. This led to secretion of large microvesicle clusters (MCs) from infected but also noninfected T cells. Noninfected cells obtained Nef through cell-to-cell contact-dependent trogocytosis and potentially by microvesicles and rapidly started secretion. While Nef-induced secretion may increase particle release, the simultaneous exocytosis of microvesicles has potentially detrimental bystander effects on noninfected cells and their immune functions.

RESULTS

Nef Alters and Accelerates T Cell Endocytosis

The downregulation of surface receptors by Nef prompted us to investigate its effect on membrane trafficking using our previously described Nef-inducible Jurkat cell line (Witte et al., 2004). The cell line expresses a Nef-estrogen-receptor fusion protein (Nef-mER) allowing assessment of Nef activity within minutes after induction by tamoxifen. To analyze membrane trafficking, we employed FM1-43, a water-soluble fluorescent styryl dye that rapidly inserts into the outer leaflet of the plasma membrane (PM) and spreads within the endosomal compartments by endocytosis (Betz et al., 1996). Jurkat cells were induced for Nef activity, and FM1-43 was added simultaneously to the medium while the cells were monitored by confocal video microscopy over a period of 20 min. In the majority of Nef-induced cells (~71%), intracellular patches of FM1-43 fluorescence were readily detectable after 5–7 min. These patches enlarged with time and grouped in the Golgi region (GR) (Figure 1A, middle panels, and Movie S2). Conversely, in ~84% of control cells, FM1-43 fluorescence appeared only after 10–15 min and presented a more scattered membrane proximal pattern (Figure 1A, upper panels, and Movie S1), likely representing early endosomes. Strikingly, T cells stimulated with PHA showed the same staining pattern (~81%) and time kinetic as Nef cells (Figure 1A, lower panels, and Movie S3).

Altered and accelerated endocytosis by Nef was also observed on the protein level when we analyzed trafficking of the transferrin receptor (TfR). TfR is found mainly in early and recycling endosomes, but accumulates in MVBs after T cell activation by PHA (Geuskens et al., 1989). Inducible Jurkat cells were stained with an anti-TfR antibody and were subsequently activated by Nef or with PHA for 30 min and analyzed by confocal microscopy. Nef-induced and PHA-activated cells displayed mostly polarized patches of TfR, typically in the GR and similar to that observed previously after Nef expression (Atkins et al., 2008; Madrid et al., 2005). Individual patches appeared in a reduced number of confocal layers and were more compact and stained brighter (Figure 1B, middle and lower panels). In contrast, control cells presented an evenly distributed, punctuate staining pattern in almost all confocal layers (Figure 1B, upper panels). Importantly, the relocalization of TfR was not due to a block of endosomal recycling, since TfR surface levels remained stable within 4 hr after Nef induction/PHA stimulation (Figure 1C).

Accelerated Endocytosis by Nef Is Linked to Exocytosis

In our live imaging analysis, intracellular FM1-43 patches that appeared in the GR also moved backward toward the PM and converted into large and bright globular structures on the cell surface (~1/cell every 2–3 min) (Figure 2A, white arrows, and Movies S5 and S6). Their appearance on the PM was significantly increased in Nef-induced (~21%) and PHA-activated (~27%) cells (Figure 2A, right graph). Typically, the stained patches moved toward a defined area of the PM or, upon cell-to-cell contact, toward the contact zone (Figure 2B, white arrows, and Movie S8). Conversely, in control cells, they appeared randomly (Figure 2B, yellow arrows, and Movie S7). In line with the secretion of large globular structures, endocytic vesicles that were prestained with FM1-43 rapidly decreased after Nef induction, and clustered vesicles were predominantly affected (Figure 2C, white arrows). Collectively, these vesicle dynamics were in agreement with polarized secretion from endocytic organelles identical to those seen in T cell activation by PHA.

Nef-Induced Exocytosis Leads to the Release of Large Clusters of Vesicles

In a previous analysis, FM1-43-stained globular structures on the PM of activated T cells (as in Figure 2A, white arrows) were identified as exosomes (Fomina et al., 2003). To test this finding, Nef cells induced for 30 min were analyzed by EM. In comparison to noninduced cells, we found a 10-fold increase of vesiculated membrane clusters on the PM, about 5–800 nm in diameter (Figures 3Ai–iv; quantification in Figure 3C). The clusters were composed of a large number of vesicles (~70 ± 10 nm; n = 30) surrounded by PM. Importantly, identical membrane clusters were detected on the surface of PHA-activated cells stimulated for 30 min (Figures 3Av and S1; quantification of the result in Figure 3C). The origin and nature of the vesicles within the clusters was not clear. While previous findings (Fomina et al., 2003) and the high content of CD63 pointed to exosomes, the unusual generation and release mechanism (see below in Figure 3B) suggested a different origin. Although we tended to believe that the vesicles were exosomes, we decided to designate them as microvesicles or MCs throughout the paper.

MCs Are Released Primarily through a Budding-like Process

By analyzing multiple EM pictures, it appeared that the Nef-induced MC release mechanism resembled a budding-like process (Figure 3B), which occurred very often (~65%) at the site of microvilli formation and protrusions as in Figure 3Ai. First, small vesicles were seemingly transported from the cytoplasm to the PM and bulged the PM into a ball-like structure (Figures 3Bi–ii). Then, the PM apparently ruptured (Figure 3Biii) and released the MCs (Figure 3Aiv), eventually leaving an empty membrane compartment behind (Figure 3Biv). Surprisingly, the released MCs remained coherent and attached in whole complexes to cell surfaces of bystander cells (Figures 3Bv and S2). In addition, MCs were also released from large vacuoles located within the cytosol, producing an opening to the extracellular space. The

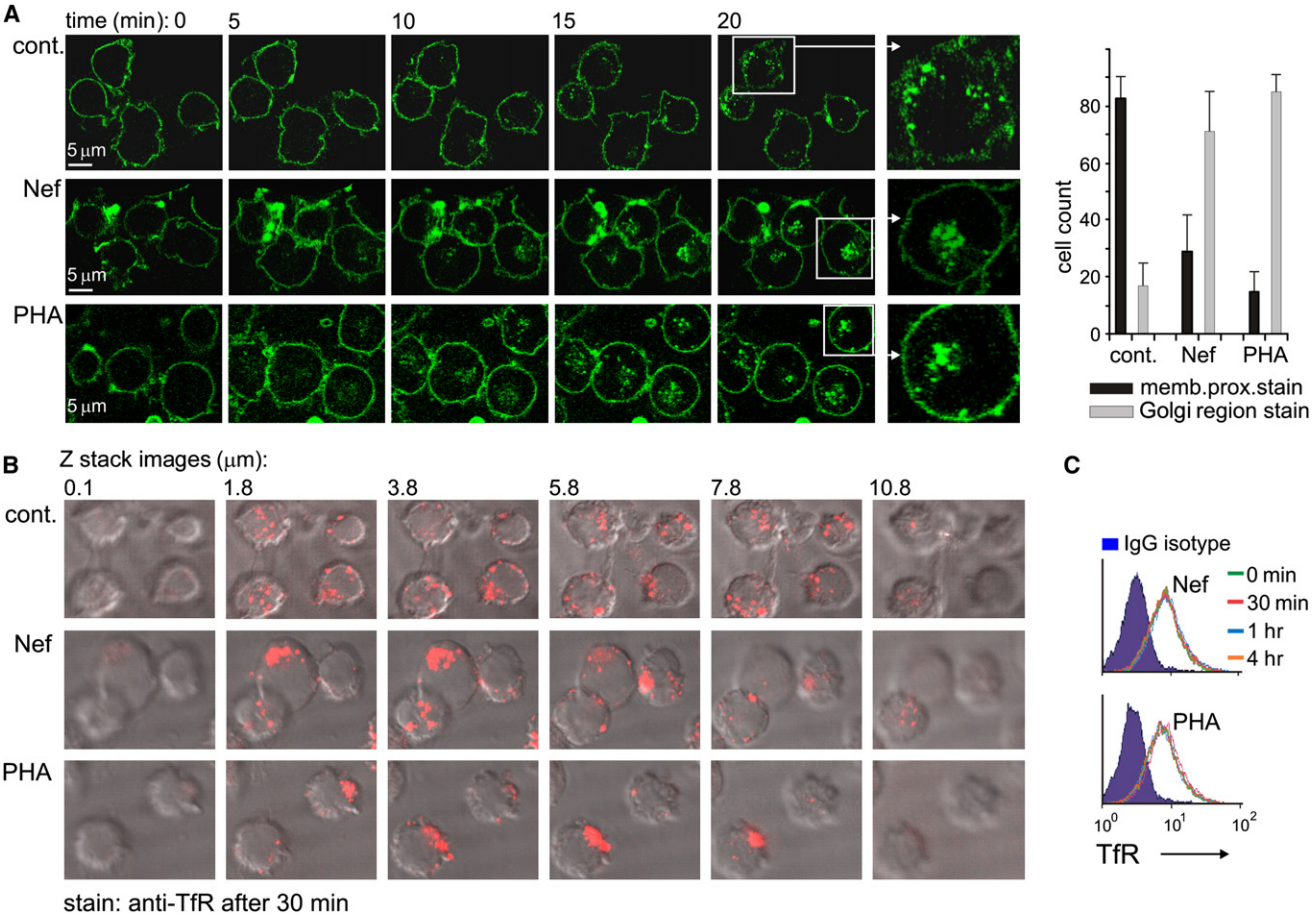

Figure 1. Transformed and Accelerated Endocytosis in Nef-Induced Jurkat Cells

(A) Individual images from confocal microscopy Movies S1–S3 (0–20 min) showing accelerated/transformed endocytosis. At time 0, FM1-43 was added to the medium of Nef-inducible Jurkats (see Experimental Procedures) along with PBS (cont.: Nef-mER expression, no Nef activity), tamoxifen (Nef: Nef-mER expression and activation), or PHA (PHA: no Nef-mER expression). Subsequently, every 15 s, a picture was taken (20 min total). For each condition, 100 cells were analyzed by live microscopy, assessing the two different endocytosis patterns as indicated (bar diagram). Error bars show means ± SD from three independent analyses.

(B) Endocytosis of TfR after stimulation with Nef or PHA. Jurkat T cells were stained with anti-TfR-PE; activated for 30 min by Nef induction, PHA stimulation (5 μg/ml), or PBS (cont.); and analyzed by confocal microscopy.

(C) Surface levels of TfR after Nef activation and PHA stimulation. Jurkat cells were induced for Nef activity or stimulated with PHA (5 μg/ml) for different time intervals before being stained with anti-TfR-PE and analyzed by FACS.

latter was similar to that expected for MVB fusion with the PM and was observed more often in PHA-stimulated cells (Figure S3). Although these images suggested that the Nef-induced generation of MCs differed from previously described mechanisms (Cocucci et al., 2009; Fomina et al., 2003; Théry et al., 2002), they implied that Nef activated a secretion process.

T Cells in HIV Cultures and CD4+ Lymphocytes from HIV Patients Generate MCs

To confirm that MC generation required Nef, CEMss cells were infected with a *nef*+ or a Δ*nef* HIV strain and analyzed by EM 72 hr after infection (as in Figure 4F). In the HIV-*nef*+ culture, MCs were detected on 64% of infected cells, as identified by budding viral particles (e.g., Figure 4A, quantification in 4D). In contrast, HIV-Δ*nef* cells were almost completely negative for MCs (1%) (Figure 4D). Thus, increased MC generation induced by HIV was strictly Nef dependent. Surprisingly, and unusual for T cells, ~28% of cells infected with a *nef*− mutant contained an increased number of endosomal vacuoles, which harbored significant numbers of HIV particles (Figure S4).

To assess the relevance of our findings for HIV infection, CD4+ T cells from 4 healthy controls and 10 HIV-infected individuals (Figure S5A) were analyzed by EM. In HIV patients with a significant viral load, MC-generating cell numbers were unexpectedly high (18%–29%) (Figure 4E, patients 1–5, black bars) and remarkably similar to the numbers seen in HIV in vitro cultures (~34%) (Figure 4F). Likewise, the morphology and release mechanism of the MC clusters seemed identical to that seen in Jurkat cells (Figure 4B). In contrast, in only one healthy control was an MC-secreting cell detected (Figure 4C). Treated patients (Figure 4E, patients 6–10) with low viral loads showed a reduced but still significant number of MC-positive cells (3%–12%).

We calculated that the probability to detect an MC in a given cell by EM was ~30%–50% (Figure S5B), indicating that the

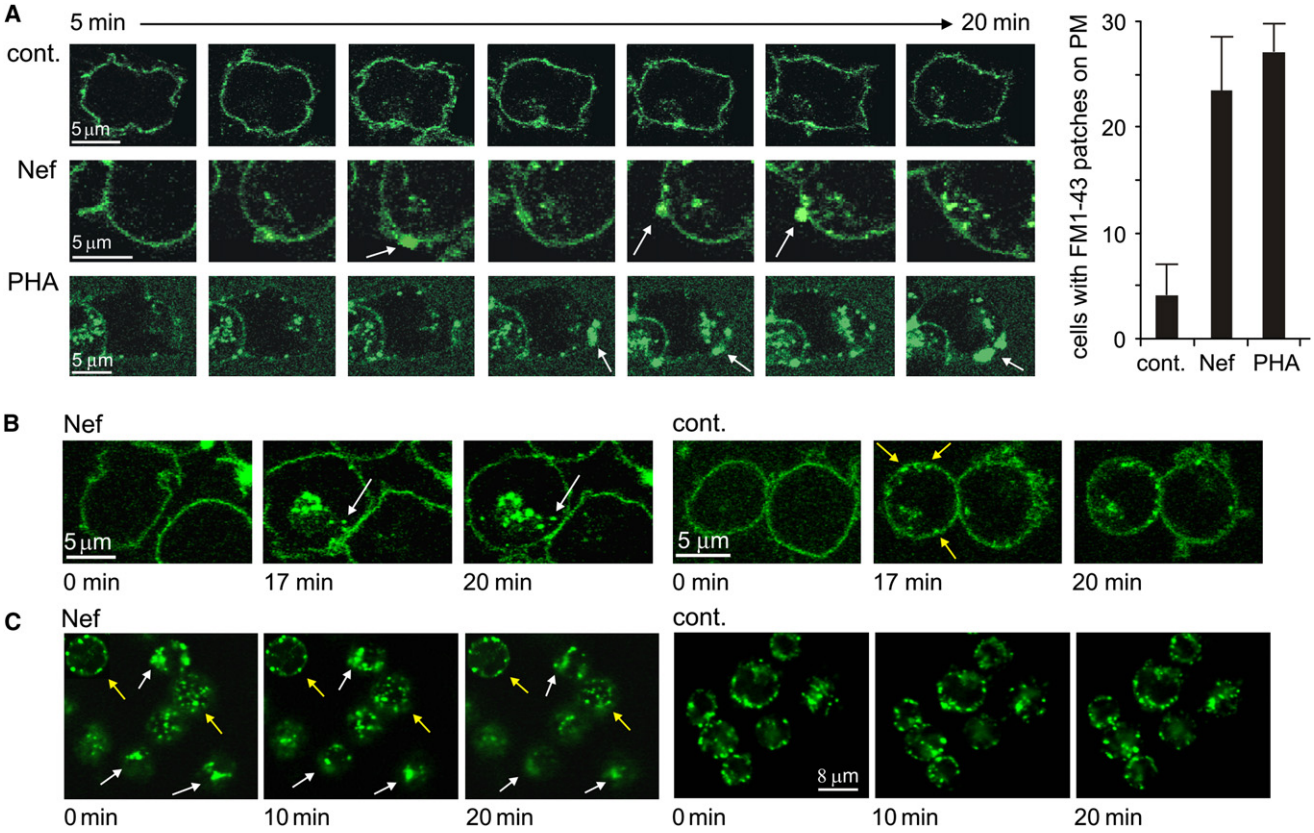

Figure 2. Nef-Induced Endocytosis Is Linked to Exocytosis

(A) Individual images from Movies S4–S6 (5–20 min) demonstrate movement and appearance of FM1-43 fluorescence patches toward/at the PM. Jurkat cells were treated as described for Figure 1A. White arrows depict the appearance of FM1-43 patches at the PM. For each condition, 100 cells were analyzed by assessing the appearance of FM1-43 membrane patches within 20 min after stimulation (bar diagram). Error bars show means ± SD from three independent analyses.

(B) Site-directed movement of FM1-43-stained vesicles toward cell-cell contact sites in Nef-induced cells, but not in noninduced controls (compare white and yellow arrows). Shown are subsequent images (0, 17, and 20 min after Nef induction from Movies S7 and S8) of Jurkat cells stimulated as described in Figure 1A.

(C) Increased exocytosis in Nef-inducible Jurkat cells demonstrated by a decrease of FM1-43-prestained vesicles. Cells were first stained with FM1-43 (4 hr, labeling the endocytic compartment), then washed and subsequently activated (Nef induction). Rapidly diminishing FM1-43 clusters are indicated by white arrows; slowly diminishing scattered vesicles are indicated by yellow arrows.

numbers of MC-generating cells were much higher. Based on these calculations, 36%–87% of circulating CD4 T cells in viraemic HIV patients generated MCs (Figure 4E, gray bars). Since most peripheral T cells are not infected, these high numbers were unexplained, but could have been caused by immune-activation mechanisms. However, in in vitro HIV cultures and thus in the absence of immune-stimulating effects, we also detected significantly more MC-positive than infected cells. For example, 72 hr after infection of CEMss cells, a representative culture showed 34% MC-positive cells as assessed by EM (68%–100% when calculated) versus 24% HIV-positive cells as assessed by intracellular FACS staining of p24 (Figure 4F). This suggested that functional Nef was transmitted to noninfected bystander cells as demonstrated previously (Qiao et al., 2006).

Nef Is Transferred to Bystander Cells by Microvesicles and Trogocytosis

To demonstrate a potential transfer of Nef onto bystander cells, we incubated Nef-RFP-expressing with GFP-expressing Jurkats in a small volume. After 90 min, ~10%–15% (n = 3) of the GFP acceptor cells revealed an additional Nef-RFP signal (Figure 5A). Upon closer examination by confocal analysis, Nef transfer occurred at cell-cell contact sites (Figure 5B, left panel) where the protein accumulated seemingly through a site-directed transport of Nef-containing vesicles (Figure 5B, right panel, white arrows), similar to that demonstrated above with FM1-43 stained patches (Figure 2B) and below (Figure 5C).

In view of the results in Figures 5A and 5B, we assumed that Nef transfer could have occurred by two different mechanisms. First, cytoplasmic Nef could have been secreted and transferred in microvesicles, as reported recently (Campbell et al., 2008). Second, PM-associated Nef, in contrast to cytoplasmic Nef, could have been transferred by the exchange of patches of PM, a mechanism termed trogocytosis (Joly and Hudrisier, 2003) and previously demonstrated for the transfer of MHC complexes (Huang et al., 1999).

The first assumption, Nef transfer by microvesicles, was supported by confocal analyses of Jurkat cells transfected with

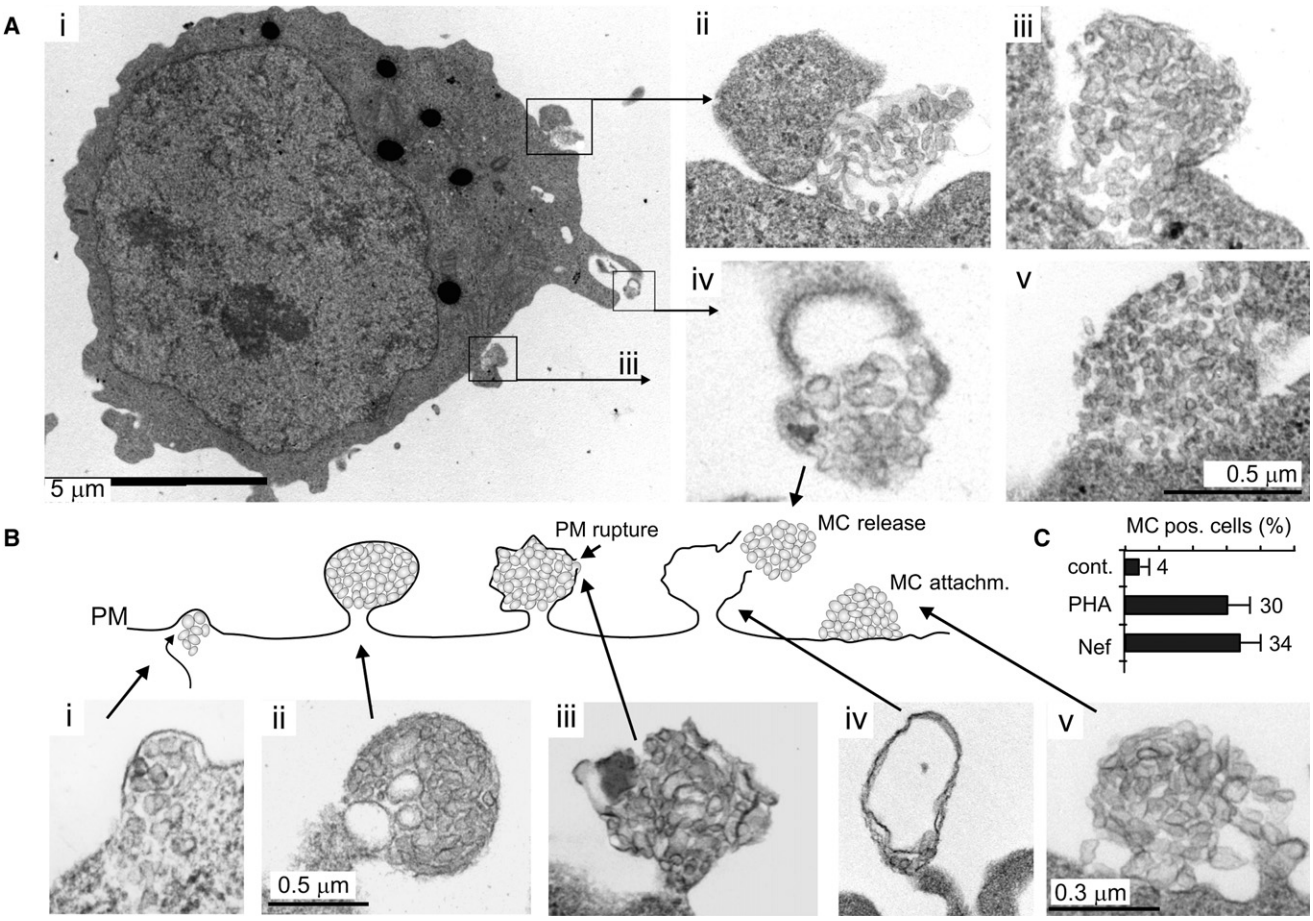

Figure 3. Nef-Induced Exocytosis Leads to the Secretion of Microvesicle Clusters at the PM of Nef-Expressing T Cells

(A) Electron micrograph of a Nef-induced (30 min) Jurkat cell (i) with three MCs emerging at the PM magnified in (ii–iv). MC released by a PHA-activated Jurkat cell is also shown (v).

(B) Subsequent stages of MC generation as described in the text (i–v).

(C) Number of MC-positive cells 30 min after Nef induction/PHA stimulation. For each condition, 100 cells were analyzed by EM. Error bars show means ± SD from two independent analyses.

Nef-GFP, revealing vesicular structures that were transported from the GR to the PM and seemingly released into the supernatant (see arrows in Figure 5C). This finding was confirmed when we purified microvesicles by a multistep centrifugation procedure (Lamparski et al., 2002) from culture supernatants of Nef-induced cells and analyzed them for the presence of Nef. In addition to previously described markers for exosomes (Blanchard et al., 2002), Nef was clearly detectable by western blot (Figure 5D, red arrow). Identical results were obtained when linear sucrose gradient fractions were analyzed accordingly (Figure 5E, upper panels), confirming the association of Nef with vesicles. Association of Nef with microvesicles was also observed in Nef-transfected immature dendritic cells (imDCs), which release microvesicles on a constant basis (Figure 5E, lower panel).

Next, we asked whether PM transfer (trogocytosis) occurred in Nef-expressing cells. We coexpressed Nef with a truncated CD8 construct (CT), which lacks the cytoplasmic domain and is highly PM-associated (data not shown). FACS and confocal microscopy revealed an efficient Nef-dependent transfer of CT onto GFP acceptor cells (Figure 6A, upper graphs). The transfer efficiency depended on the number of CT donor cells, but reached a saturation point (1:2 donor/acceptor ratio), suggesting that cell-cell contact was the limiting factor. Importantly, the same effect was seen with PHA-stimulated donor cells (Figure 6A, lower graphs), implying that trogocytosis, like MC secretion, was a function of T cell activation. Upon closer examination, Nef-expressing cells seemed to embrace GFP acceptor cells with filopodia at the contact site (Figure 6B, upper panels; see also Figure 5B), which eventually pinched off and remained on the surface of the target cell (lower panels), as described previously (Williams et al., 2007).

To assess whether Nef-mediated trogocytosis was functional and would transfer signaling competent receptors/molecules, a CD8-ζ (derived from TCR-ζ) fusion protein was coexpressed with Nef in donor cells, while acceptor cells received an NFAT-luciferase reporter. After coincubation, transferred CD8-ζ was activated by α-CD8 crosslinking. As shown in Figure 6C, luciferase activity increased in acceptor cells in a strictly Nef-dependent manner. Collectively, these results demonstrated that cell-to-cell contact-dependent trogocytosis and potentially

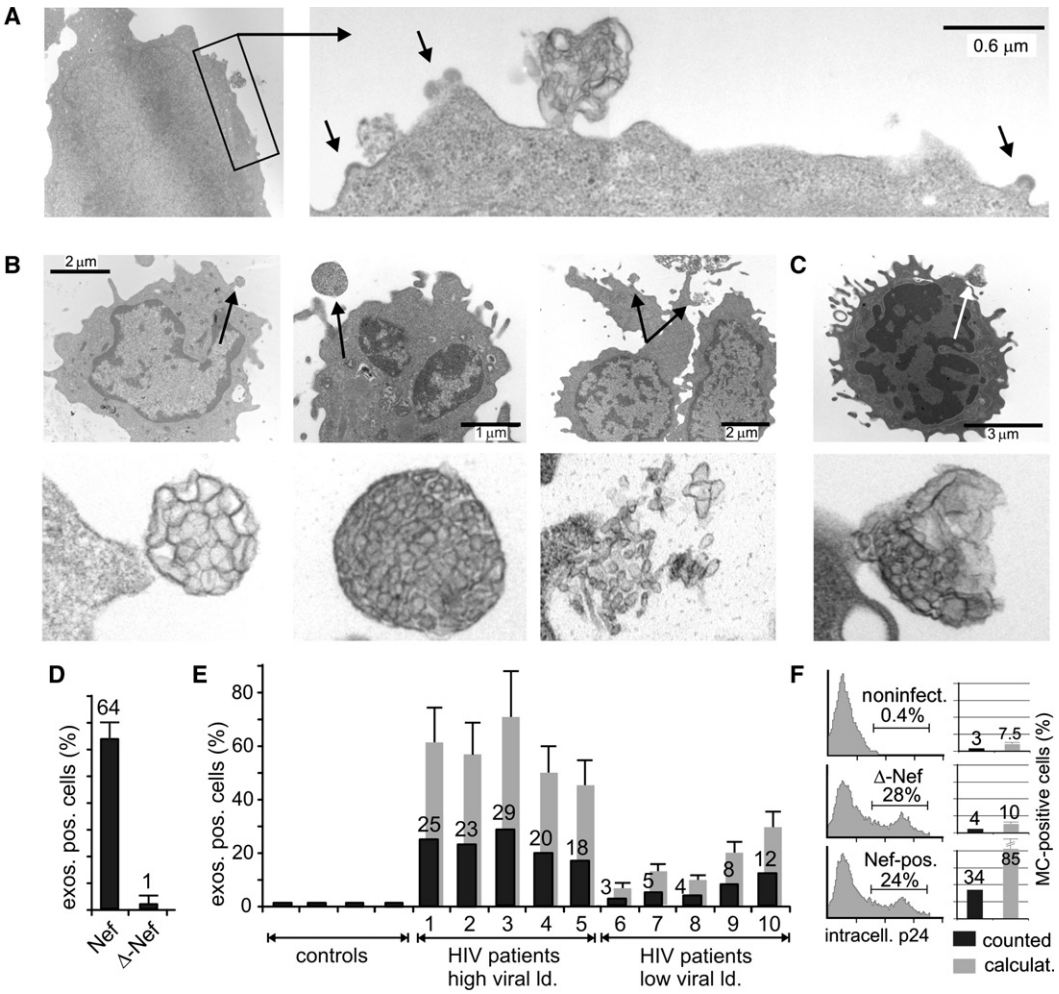

Figure 4. MC Secretion from HIV-Infected Cells In Vitro and Primary CD4 Lymphocytes

(A) Protruding MC on the PM of an HIV-infected CEMss cell. Arrows depict budding viral particles. Cells were analyzed 3 days after infection.

(B and C) EM pictures of MC-secreting primary T cells taken from three infected individuals (pat. 1, 2, and 4 in Figure 4E) and one healthy control (C).

(D) MC secretion is Nef dependent. CEMss cells were infected with a nef+ and a Δnef-NL43 strain. Shown are the numbers for 50 visibly infected cells as determined by budding viral particles assessed through EM 3 days after infection. Error bars show means ± SD from three independent analyses.

(E) MC-secreting primary T cells out of 100 analyzed for ten HIV-infected individuals (details in Figure S4A) and four healthy controls. Black bars represent EC-positive cells assessed by EM, and gray bars the projected numbers based on calculation (see Figure S4B). Error bars show the possible ± SD of calculated numbers as explained in Figure S4A.

(F) Actual and calculated numbers of EC-positive cells in an HIV in vitro culture. HIV-positive cells were determined by p24 FACS 3 days after infection (histograms). EC-positive cells were determined by EM (black bars) or calculated as described in Figure S4B (gray bars including error bars).

microvesicles caused the transfer of Nef and activated signaling complexes onto bystander cells.

Nef Induces Secretion of FasL

Since conventional detection systems for secreted microvesicles are lacking, we were looking for an additional marker that would confirm Nef-induced secretion and could be assayed more easily. One of the best studied markers secreted on vesicles from activated CD4 T cells is FasL (Andreola et al., 2002; Bossi and Griffiths, 1999; Jolly and Sattentau, 2007; Martínez-Lorenzo et al., 1999). First, we analyzed purified vesicle preparations from Nef-induced Jurkat cells for the presence of FasL by FACS. In addition to reported surface markers like CD63 (Blanchard et al., 2002), a subfraction of microvesicles (18%) displayed an unusual bright FasL signal that was also detected on PHA-induced microvesicles but not on the PM of Jurkat cells (Figure 7A, see arrows). In accordance with this finding, intracellular FasL stores were significantly reduced after Nef induction or PHA stimulation (Figure S6), as reported previously (Andreola et al., 2002; Monleón et al., 2001).

The copresence of Nef and FasL in microvesicles implied that both proteins were packaged into compartments bound for exocytosis. In resting Jurkat T cells, FasL was not found in transport-associated compartments (e.g., late endosomes), as evidenced by the lack of colocalization with Rab proteins contained therein (Rab4, 5, 7, 11) (Savina et al., 2002; Seachrist and Ferguson, 2003) (Figure S7). However, after coexpression of Nef, FasL relocalized to the GR and colocalized with Rab4, 5, and 11 and

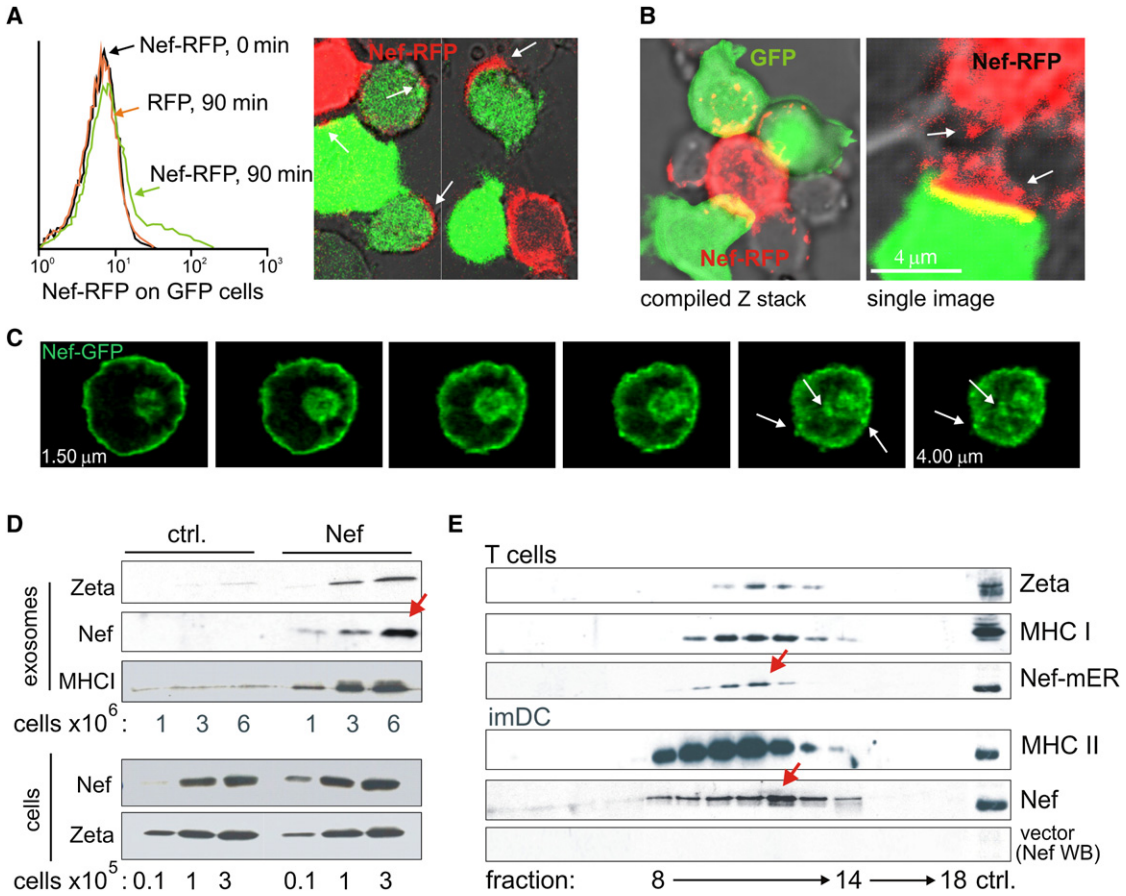

Figure 5. Transfer of Nef to Bystander Cells

(A) Detection of Nef-RFP on GFP-transfected Jurkat cells by FACS and confocal microscopy (white arrows). Transfected cells (transfection efficiency 70%–75%) were mixed at a ratio of 1:1 for 90 min. For control, RFP-transfected cells were incubated with GFP acceptor cells.

(B) Confocal images of the experiment described in (A).

(C) Confocal Z stack analysis of one Nef-GFP-expressing Jurkat cell.

(D) Western blot analysis of Nef-induced microvesicles. Microvesicles were purified as described previously (Lamparski et al., 2002). Aliquots corresponding to 1, 3, and 6 million Nef-induced Jurkats were analyzed for TCR-ζ, MHCI, and Nef-mER (upper three panels). For comparison, lysates from the producing cells were analyzed accordingly (lower panels).

(E) Western blot analysis of microvesicles purified by sucrose gradient from culture supernatants of Nef-inducible Jurkats (upper panels) or immature dendritic cells (imDCs) transfected with Nef mRNA (lower panels). Western blot signals were detected in fractions with a sucrose density of 1.13–1.19 g/ml as determined by densitometry.

Nef. A similar effect was seen upon PHA stimulation (Figure S7). For confirmation, the analysis was repeated in transfected 293T cells. Again, upon coexpression of Nef, FasL relocalized to the GR and colocalized there with Rab4, Rab11, and Nef (Figure 7B, see arrow, and Figure S8). Together, these data confirmed that Nef activated exocytosis. Obviously, this included the active packaging of FasL into secreting compartments, identical to that seen after T cell activation.

Nef Transfer to Bystander Cells Induces Transsecretion of FasL

Next, we asked whether Nef protein transduction would transfer Nef-induced FasL secretion to bystander cells, which could explain the high numbers of secreting cells found in HIV-infected individuals. For practical reasons, we termed this assumed mechanism "transsecretion." We designed a simple transsecretion assay as depicted in Figure 7C, scoring for FasL in the supernatant by CBA (cytokine bead array). We transfected 293T cells with Nef or control DNA and sedimented Jurkat cells on top by adding them to the culture dish. In order to avoid cell killing by the released FasL, the Jurkats were transfected with a FasL point mutant unable to bind Fas. After 12 hr of coincubation, the supernatant was assayed for FasL. As demonstrated in Figure 7B, Nef induced significant transsecretion of FasL, which equaled about 20% of the amount measured in the positive control (20 μg PHA for 12 hr).

For further confirmation, we asked whether transsecretion could be demonstrated in primary CD4 T cells. We reasoned that transsecreting CD4 cells should express CD107a, which is an established degranulation marker. We repeated the assay depicted in Figure 7C, replacing Jurkats with PBMC blasts (see Experimental Procedures for details). Since secretion is rapidly

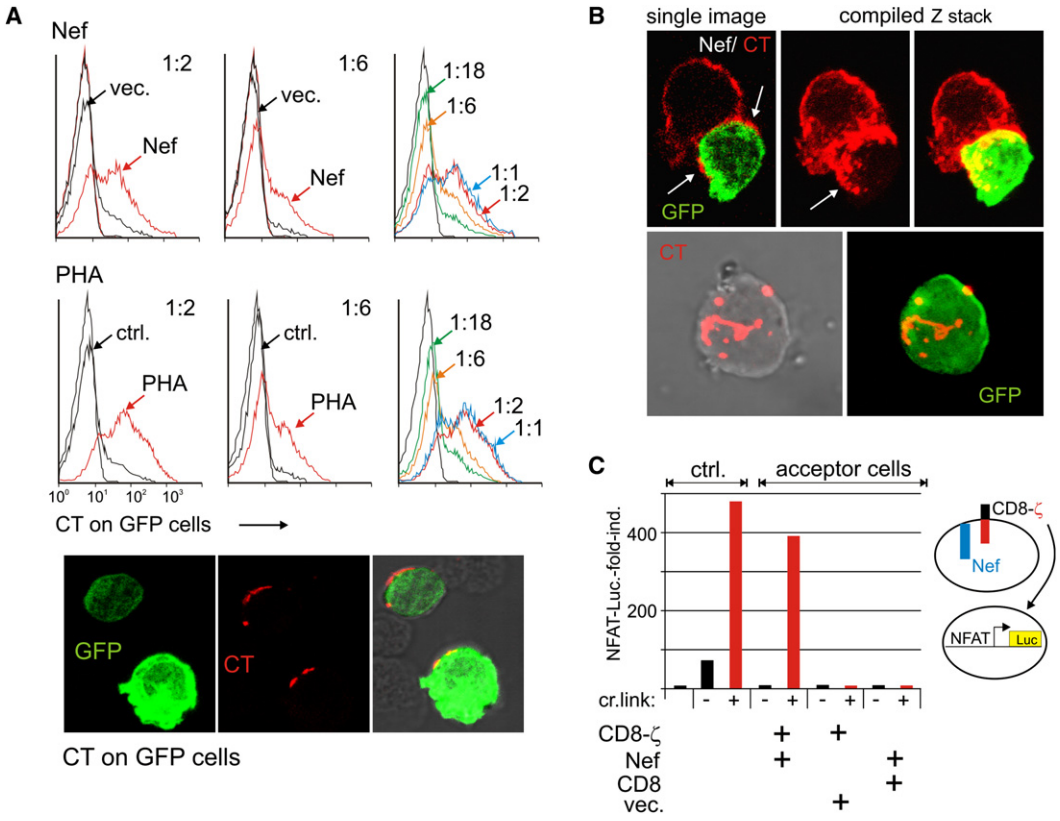

Figure 6. PHA-Activated and Nef-Expressing Cells Induce Trogocytosis

(A) Detection of truncated CD8 (CT) on GFP acceptor cells by FACS analysis and confocal microscopy. Donor cells transfected with CT and Nef or control vector (vec.) (upper graphs; transfection efficiency: 70%–75%), transfected with CT and stimulated with PHA, or left untreated (ctrl.) (lower graphs) were incubated (4 hr) with GFP-transfected acceptor cells at different ratios as indicated.

(B) Transfer of CT from Nef donor onto GFP acceptor cells by filopodia (see text).

(C) Activation of NFAT in acceptor cells after Nef-induced transfer of CD8-ζ. Donor cells were transfected with CD8-ζ and Nef or controls while acceptor cells were transfected with an NFAT-luciferase reporter (see cartoon). After 4 hr of incubation, cells were crosslinked by α-CD8 and incubated an additional 6 hr before luciferase activity was measured. For system control (ctrl.), Jurkats were transfected with CD8-ζ and NFAT-Luc and crosslinked with α-CD8 as described above. Shown is one representative experiment of four performed.

induced, coincubation with Nef-transfected 293T cells was reduced to 2 hr. Thereafter, the PBMC were stained for CD4 and CD107a and analyzed by FACS. As shown in Figure 7D, about 20% of the CD4 T cells displayed CD107a and showed a secretion phenotype similar to PHA-stimulated PBMC blasts (20 μg PHA for 2 hr).

Nef-Induced Transsecretion Is Erk1/2-Dependent

T cell secretion is a signaling-induced process mediated by Erk1/2, PKCθ, and PI3 kinase (Berg et al., 1998; Puente et al., 2006; Robertson et al., 2005). We have recently reported that Nef activates these three kinases through formation of an hnRNPK-dependent signaling complex (Witte et al., 2008; Wolf et al., 2008a, 2008b). Both observations implied that the Nef-associated hnRNPK complex activated secretion. In fact, in our Nef transsecretion assay, an inhibitor of Erk1/2 (U0126) potently blocked FasL release from Jurkat cells (Figure 7E). Confirming these findings, a Nef mutant (CD8-Nef fusion protein) unable to activate Erk1/2 (CNΔ11-40) (Wolf et al., 2008b) failed to induce FasL release (Figure 7E). U0126 also blocked PHA-induced secretion, implying that the Nef-hnRNPK complex stimulated the same secretion pathway activated by the TCR (Figure 7E). This was expected, since (1) we found no phenotypical or functional difference between Nef- and PHA-induced secretion (Figures 1–3) and (2) we had demonstrated that the hnRNPK-dependent signaling complex also formed after TCR activation (Wolf et al., 2008b). Collectively, these assays confirmed our assumption that Nef transfer to bystander cells induced an Erk1/2-dependent signaling pathway that caused T cell secretion.

DISCUSSION

In this report, we suggest that Nef-activated membrane trafficking is bidirectional and identical to that in activated T cells. Phenotypical hallmarks of this process are a sustained microvesicle secretion and an induction of PM transfer (trogocytosis). The physiological functions of both processes are not known, and therefore their role in HIV infection and pathogenesis remain unclear for now. However, in addition to other mechanisms (Sowinski et al., 2008), these events may lead to the efficient spreading of Nef and Nef-induced activation events to bystander

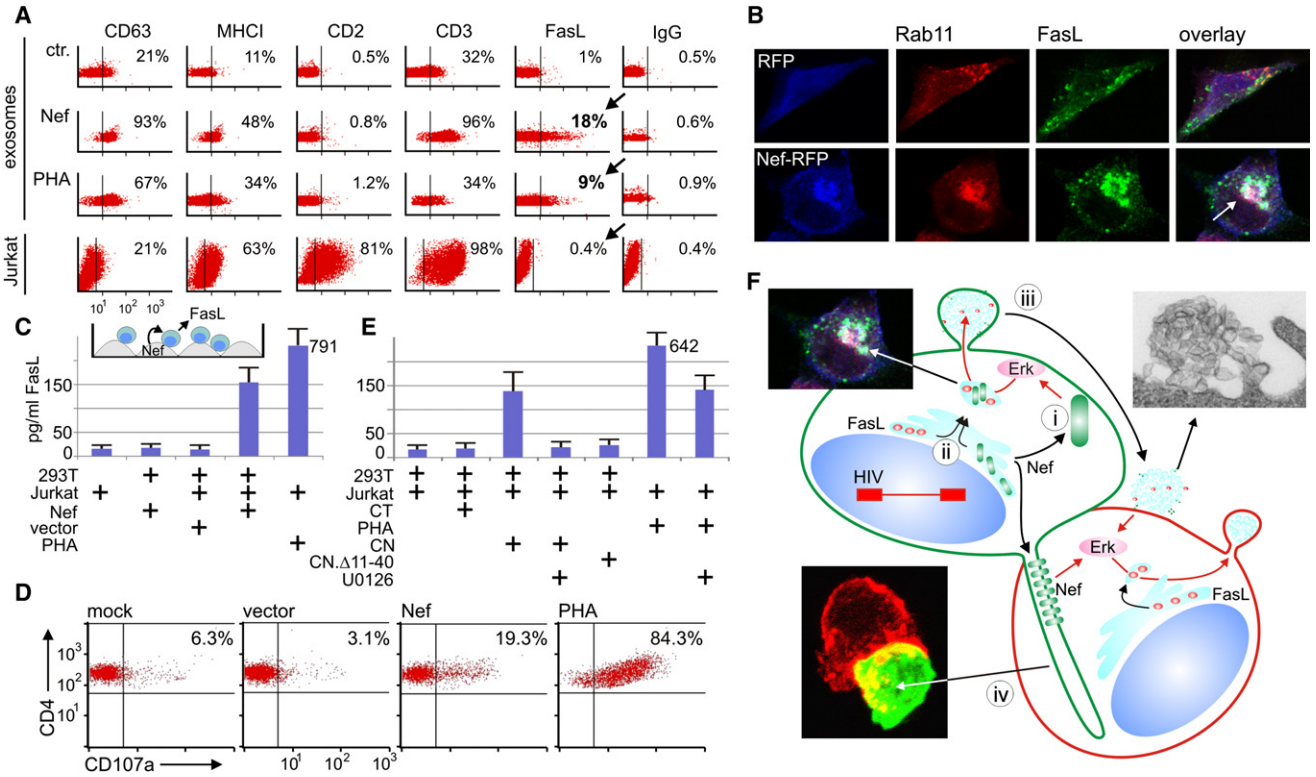

Figure 7. Nef Transfer to Bystander Cells Induces Secretion of FasL

(A) Microvesicles from Nef/PHA supernatants were analyzed by FACS. For comparison, the secreting Jurkat cells were analyzed accordingly (lower graphs).

(B) Confocal analysis of 293T cells transfected either with RFP or Nef-RFP along with FasLY218A (unable to bind Fas) and Rab11-GFP as indicated. Note that colors were changed for better analysis.

(C) Nef induces FasL transsecretion. Nef-transfected 293T cells were incubated for 12 hr with FasLY218A-transfected Jurkat cells, as depicted in the cartoon, before supernatants were assayed for FasL by cytokine bead array (CBA). Jurkats stimulated with PHA (20 μg/ml, 12 hr) served as control. Values represent the mean ± SD of three independent experiments, each performed in duplicate.

(D) PBMC blasts (see Experimental Procedures) incubated for 2 hr with Nef-transfected 293T cells were analyzed for CD107a and CD4 by FACS. Controls were stimulated with PHA (20 μg/ml, 2 hr).

(E) Nef-induced transsecretion is Erk1/2 dependent. 293T transfected with CD8-Nef chimeras were incubated with Jurkats in the presence/absence of an Erk-inhibitor (U0126). Supernatants were assayed for FasL after 12 hr. Values represent the mean ± SD of three independent experiments, each performed in duplicate.

(F) Proposed model of transfer of infected cell signaling (TOS) by HIV. Nef expression (i) induces the activation of an Erk1/2-dependent secretion pathway, which causes (ii) the packaging of FasL and Nef into secreting compartments, (iii) the secretion and attachment of MC to bystander cells, and (iv) the induction of trogocytosis. This leads to the transfer of Nef and induction of secretion in bystander cells.

cells. This could explain our observation that most noninfected CD4 T cells in viraemic HIV patients display a secretion phenotype, which likely affects their functions and contributes to immunodeficiency.

The mechanistic connection between Nef-mediated receptor endocytosis and HIV pathogenesis is difficult to understand, in part because many receptors are affected and some, like CD8, are generally not found on infected cells. In activated T cells, like in other stimulated cells, endocytosis and exocytosis are coordinated events that ensure a balanced cycling of membranes (Gundelfinger et al., 2003; Morris and Homann, 2001). Therefore, increased endo- and exocytosis are two sides of the same coin, and T cell secretion could be the pathogenesis-relevant process caused by Nef. The latter would help to explain the detrimental *trans*-effect on noninfected cells seen in HIV infection. Likewise, the seemingly separate actions of Nef, activation of TCR signaling (Baur et al., 1994; Simmons et al., 2001) and receptor endocytosis (Garcia and Miller, 1991), may serve one function, namely the activation of membrane trafficking. In line with this assumption, a Nef mutant defective for Nef signaling (CNΔ11-40) was unable to stimulate transsecretion.

There is ample evidence that polarized secretion toward cell-cell contact sites increases the spread of HIV infection (Fais et al., 1995; Haase, 2005; Johnson and Huber, 2002; Jolly and Sattentau, 2007; Pearce-Pratt et al., 1994). Similarly, HTLV-I induces polarization of the cytoskeleton for optimal cell-to-cell transmission (Igakura et al., 2003). It is likely that Nef-activated secretion assists this process, guiding viral proteins to cell-cell contact sites. Several observations support this assumption. First, we noticed that cells infected with a *nef*− mutant contained compartments with viral particles. The latter is unusual for T cells (Ono and Freed, 2001; Pelchen-Matthews et al., 2003) and could be explained by the lack of polarized secretion. Second, optimal particle release required Nef-induced cytoskeleton rearrangements (Fackler

et al., 1999; Lu et al., 1996). Third, gag and env proteins are transported to the PM by a Nef-dependent process (Argañaraz et al., 2003; Dong et al., 2005; Sandrin and Cosset, 2006; Schiavoni et al., 2004). In summary, Nef-induced exocytosis may facilitate viral protein transport in a site-directed manner for optimal cell-to-cell transmission.

As shown here, Nef transduction includes the transfer of Nef-associated signaling activities to bystander cells. Recent publications support our findings demonstrating the presence of signaling-competent Nef in B cells (Qiao et al., 2006), the transfer of HIV viral proteins by nanotubes (Sowinski et al., 2008), and the transfer of Nef by vesicles (Campbell et al., 2008). Together with our report, a picture of HIV infection emerges that seems to involve bystander cells, potentially with a specific functional role in the viral life cycle. Since the viral protein transfer is efficient and functional, this mechanism may be best described as transfer of infected cell signaling, or TOS (Figure 7F). Interestingly, a comparable viral protein transfer has been described previously for vp22 and HSV-1 (Elliott and O'Hare, 1997), although it did not seem to involve cell signaling.

What could be the relevance of TOS for the viral life cycle? At present, this is not clear, but we have obtained data pointing to a role in HIV replication (K.K., unpublished data). Here, we demonstrate that at least a fraction of the T cell-derived vesicles contained FasL. We would therefore speculate that MCs, with their high density of surface receptors, affect target cells in multiple ways, and induction of apoptosis by FasL could be one consequence, for example to fight off attacking CD8 cells. The latter would be in line with previous findings in monkeys, correlating Nef-induced FasL upregulation with immune escape from CTL (Xu et al., 1997).

In summary, our report supports the assumption that immune dysfunction in HIV infection is caused by nonphysiological T cell stimulation and suggests that extensive MC secretion has detrimental bystander effects.

EXPERIMENTAL PROCEDURES

The Nef-Inducible Cell Line

Previously, we described a Jurkat cell line that is inducible for a Nef-estrogen receptor fusion protein (Nef-mER) (Witte et al., 2004). Briefly, a fusion protein between Nef and the tamoxifen-sensitive mutant of the estrogen receptor (Nef-mER) was cloned under the control of a tetracyline-inducible system (Invitrogen), and a stable cell line was established. Addition of doxycyclin (dox) (overnight) results in expression of an inactive Nef protein with minor background Nef activity, whereas addition of tamoxifen (tam) activates Nef within minutes (Witte et al., 2004).

Cells, Antibodies, and mRNA Transfection

The Nef-inducible Jurkat cell line (Jurkat Nef-mER) was cultured in RPMI 1640 supplemented with 10% FBS (GIBCO; Carlsbad, CA). 293T cells were cultured in Dulbecco's minimal essential medium supplemented with 10% FBS. ImDC differentiation and electroporation with mRNA were performed essentially as described previously (Schaft et al., 2005). Briefly, CD4 T cells were washed once with RPMI and once with PBS at RT and resuspended to a final concentration of 40×10^6 cells/ml in phenol-free Opti-MEM medium (GIBCO). Subsequently, 200 μl of the cell suspension was mixed with 10 μg of in vitro transcribed mRNA and electroporated by a Bio-Rad Gene Pulser Xcell with square wave program at 500V for 0.5 ms in a 0.4 cm cuvette.

Anti-CD71 antibody (DF1513; Santa Cruz Biotechnology; Santa Cruz, CA); anti-FasL (NOK1, G247-4; BD Pharmingen; San Diego, CA); anti-ζ chain (6B10; Biocarta; San Diego, CA); anti-HLA-A,B,C (G46-2.6; DAKO; Glostrup, Denmark); anti-HLA-DR (TAL.1B5; DAKO); anti-CD63, anti-CD45, anti-CD2, and anti-CD3 (BD PharMingen); anti-CD107a (H3A4, BD Biosciences; San Jose, CA); Alexa Fluor 488/647-conjugated goat anti-mouse IgG (Molecular Probes; Carlsbad, CA); and anti-AU-1 (BAbCO; Richmond. CA) were used according to the manufacturers' instructions. The sheep anti-Nef serum was kindly provided by M. Harris (Leeds) and used at a 1:5000 dilution.

Transsecretion and CD107a Degranulation Assay

293T transfected cells (2×10^5) (Nef, empty vector, CD8-Nef [CN], CNΔ11-40, CT [CD8 truncated], see Wolf et al., 2008b for details) were seeded into a 96-U-bottom well. Subsequently, 1×10^5 Jurkat cells, which had been transfected 24 hr before with FasL mutant FasLY218A, unable to bind Fas, were added. After 12 hr of coincubation, cell-free supernatants were assayed for FasL by CBA (BD Biosciences) according to the manufacturers' procedures. For positive control, 1×10^5 Jurkats were stimulated with PHA (20 μg/ml) for 12 hr.

To assay CD107a on primary CD4 bystander cells, fresh PBMCs were stimulated overnight with 1 μg/ml PHA, washed, and cultivated with IL-2 (10 U/ml) for 3 more days. Thereafter, and for each condition, 5×10^5 PBMC blasts were taken up in Monensin (2 μM) and 10 μl of CD107a-FITC antibody and placed on top of 4×10^5 transfected 293T cells in a 48-well plate (total volume 100 μl). Cells were coincubated for 2 hr before PBMCs were harvested, washed, stained with CD4-PE, and analyzed for CD4 and CD107a by FACS. For positive control, PBMC blasts were stimulated with PHA (20 μg/ml) for 2 hr and analyzed accordingly.

Virus Preparations and Infections

Production of viral particles and infection of CEMss were essentially performed as described previously (Schiavoni et al., 2004). All HIV-1 molecular clones (WT and Δ*nef*) were derivates of the NL4-3 strain. Virus stocks were obtained from transiently transfected 293T cells. Briefly, 293T cells were transfected with 30 μg of proviral DNA by calcium phosphate/DNA coprecipitation. Supernatants were harvested 48 hr after transfection, laid on top of a 20% sucrose cushion, and centrifuged at 100,000 *g* for 2 hr. Virus preparations were titrated by both anti-p24 Gag quantitative ELISA (Abbott; Abbott Park, Illinois) and reverse transcriptase assay. Infections of CEMss were performed by absorbing the virus inoculum onto cell pellets for 1 hr at 37°C. Infection efficiency was evaluated 72 hr after infection by p24 intracellular FACS staining.

FM1-43 Staining and Video Microscopy

Nef-inducible Jurkat cells were placed on poly-L-lysine-coated Lab-Tek II chambered glass slides (Fisher Scientific; Schwerte, Germany) covered with 500 μl of RPMI 10% FBS. Subsequently, 3.5 μM FM1-43 (Molecular Probes) was added along with tamoxifen, PBS, or 5 μg/ml PHA. Images were taken by time-lapse video fluorescence microscopy using a Video (Spinning Disk) Confocal Microscope (CARV) equipped with a Zeiss Axiovert 200 microscope, 10–66×. For FM1-43 excitation, light was filtered with a 485/506 nm and emitted light was collected with a 595/750 nm bandpass filter. Images were acquired with a 2 × 2 binning at a rate of 1 frame every 15 s.

Immunofluorescence

Jurkat Nef-mER cells were placed on poly-L-lysine-coated cover glass. Cells were fixed in 4% paraformaldehyde (Sigma; St. Louis), quenched for 10 min with 0.1 M glycine in PBS, and permeabilized with 0.1% Triton X-100 (Sigma) in PBS. Cells were then blocked with 1% BSA and stained with the respective antibodies. In the TfR internalization assay, Jurkat Nef-mER cells were first stained with an anti-TfR antibody (4°C) followed by a Texas Red-coupled anti-mouse IgG secondary antibody (4°C). Cells were then induced for Nef activity or stimulated with 5 μg/ml PHA and cultured at 37°C for the times indicated. Cells were finally placed on polylysine-coated cover glass, fixed, and analyzed using a Zeiss LSM 510 Confocal Laser Scanning Microscope (CLSM).

FACS Analysis of Cells

One hundred thousand cells were washed twice in FACS buffer (2.5% FBS in PBS) and stained with the respective antibodies. Intracellular staining of FasL was performed by permeabilizing cells with 70% methanol (−20°C for 30 min) followed by anti-FasL (G247-4) or FITC-conjugated anti-mouse IgG staining. Cells were analyzed using a FACSCalibur flow cytomer (BD Biosciences)

and CELLQuest software (BD Biosciences). Quantitative assessment of apoptosis was performed by Annexin-V staining (BD PharMingen) 15–24 hr after incubation with exosomes.

Isolation and Purification of Microvesicles

Microvesicle purification was conducted as previously described (Raposo et al., 1996). Briefly, cellular supernatants from 40 × 10^6 Jurkat Nef-mER cells were collected 24 hr after Nef induction and PHA activation (1 μg/ml). Supernatants were centrifuged for 20 min at 1,200 *g*, 30 min at 10,000 *g*, and 1 hr at 100,000 *g*. Pellets were resuspended in 30 ml PBS and centrifuged again at 100,000 *g* for 1 hr. Pellets were solubilized in 50 μl PBS and considered as exosome preparations. For further purification, exosome pellets were resuspended in 5 ml of 2.5 M sucrose, 20 mM HEPES/NaOH [pH 7.2], and a linear sucrose gradient (2–0.25 M sucrose, 20 mM HEPES/NaOH [pH 7.2]) was layered on top of the microvesicle suspension. The samples were then centrifuged at 100,000 *g* for 15 hr. Gradient fractions were collected, diluted in 3 ml PBS, and ultracentrifuged for 1 hr at 100,000 *g*. Pellets were solubilized in SDS sample buffer and analyzed by SDS-PAGE and western blotting.

FACS Analysis of Microvesicles

FACS analysis of bead-coupled microvesicles was performed as previously described (Blanchard et al., 2002). Briefly, microvesicles prepared from cell supernatants were incubated with 5 μl of 4 μm diameter aldehyde/sulfate latex beads (Interfacial Dynamics; Portland, OR) in a final volume of 20 μl for 15 min at RT; 10 μg BSA was then added to each sample and incubated for 15 min. This step was followed by a 75 min incubation period in 1 ml PBS with gentle shaking. Microvesicle-coated beads were washed twice in FACS buffer and resuspended in 400 μl FACS buffer. Microvesicle-coated beads (30 μl) were incubated with each antibody, followed when necessary by incubation with a FITC-conjugated antibody, and analyzed by FACS.

Transmission Electron Microscopy

For transmission electron microscopy (TEM), cells were fixed in 0.1 M sodium cacodylate buffer containing 2.5% glutaraldehyde (pH 7.2) at RT for 20 min. After washing three times in 0.1 M sodium cacodylate, cells were postfixed in 1% osmium tetroxide in the same buffer. After 1 hr of incubation at RT, cells were dehydrated through a graded series of ethanol solutions and finally embedded in Agar 100 epoxy resin. Thin sections were stained with lead citrate and uranyl acetate and examined with a Philips 208 s electron microscope.

SUPPLEMENTAL DATA

Supplemental Data include eight figures and eight confocal microscopy movies and can be found online at http://www.cell.com/cell-host-microbe/supplemental/S1931-3128(09)00282-0.

ACKNOWLEDGMENTS

We thank Beata Frydel for the excellent technical support with the confocal microscope and Elisa Vicenzi for providing PBMC samples from HIV-infected individuals. This work was supported by funds from the Department of Microbiology and Immunology, University of Miami, Miller School of Medicine (grants to A.S.B.) and the German Science Foundation (DFG), SFB 466 (C.M.) and SFB 643 (K.K.). L.E.C. and E.A.M. are supported by NIH grant CA75918. We thank Eckhard Podack for his generous support of this study.

Received: July 17, 2008
Revised: April 23, 2009
Accepted: June 26, 2009
Published: September 16, 2009

REFERENCES

Aiken, C., Konner, J., Landau, N.R., Lenburg, M.E., and Trono, D. (1994). Nef induces CD4 endocytosis: requirement for a critical dileucine motif in the membrane-proximal CD4 cytoplasmic domain. Cell *76*, 853–864.

Andreola, G., Rivoltini, L., Castelli, C., Huber, V., Perego, P., Deho, P., Squarcina, P., Accornero, P., Lozupone, F., Lugini, L., et al. (2002). Induction of lymphocyte apoptosis by tumor cell secretion of FasL-bearing microvesicles. J. Exp. Med. *195*, 1303–1316.

Argañaraz, E.R., Schindler, M., Kirchhoff, F., Cortes, M.J., and Lama, J. (2003). Enhanced CD4 down-modulation by late stage HIV-1 nef alleles is associated with increased Env incorporation and viral replication. J. Biol. Chem. *278*, 33912–33919.

Atkins, K.M., Thomas, L., Youker, R.T., Harriff, M.J., Pissani, F., You, H., and Thomas, G. (2008). HIV-1 Nef binds PACS-2 to assemble a multikinase cascade that triggers major histocompatibility complex class I (MHC-I) down-regulation: analysis using short interfering RNA and knock-out mice. J. Biol. Chem. *283*, 11772–11784.

Baur, A., Garber, S., and Peterlin, B.M. (1994). Effects of CD45 on NF-kappa B. Implications for replication of HIV-1. J. Immunol. *152*, 976–983.

Berg, N.N., Puente, L.G., Dawicki, W., and Ostergaard, H.L. (1998). Sustained TCR signaling is required for mitogen-activated protein kinase activation and degranulation by cytotoxic T lymphocytes. J. Immunol. *161*, 2919–2924.

Betz, W.J., Mao, F., and Smith, C.B. (1996). Imaging exocytosis and endocytosis. Curr. Opin. Neurobiol. *6*, 365–371.

Birch, M.R., Learmont, J.C., Dyer, W.B., Deacon, N.J., Zaunders, J.J., Saksena, N., Cunningham, A.L., Mills, J., and Sullivan, J.S. (2001). An examination of signs of disease progression in survivors of the Sydney Blood Bank Cohort (SBBC). J. Clin. Virol. *22*, 263–270.

Blanchard, N., Lankar, D., Faure, F., Regnault, A., Dumont, C., Raposo, G., and Hivroz, C. (2002). TCR activation of human T cells induces the production of exosomes bearing the TCR/CD3/zeta complex. J. Immunol. *168*, 3235–3241.

Bossi, G., and Griffiths, G.M. (1999). Degranulation plays an essential part in regulating cell surface expression of Fas ligand in T cells and natural killer cells. Nat. Med. *5*, 90–96.

Campbell, T.D., Khan, M., Huang, M.B., Bond, V.C., and Powell, M.D. (2008). HIV-1 Nef protein is secreted into vesicles that can fuse with target cells and virions. Ethn. Dis. *18*, S2–14–19.

Chaudhry, A., Das, S.R., Hussain, A., Mayor, S., George, A., Bal, V., Jameel, S., and Rath, S. (2005). The Nef protein of HIV-1 induces loss of cell surface costimulatory molecules CD80 and CD86 in APCs. J. Immunol. *175*, 4566–4574.

Cocucci, E., Racchetti, G., and Meldolesi, J. (2009). Shedding microvesicles: artefacts no more. Trends Cell Biol. *19*, 43–51.

Craig, H.M., Pandori, M.W., and Guatelli, J.C. (1998). Interaction of HIV-1 Nef with the cellular dileucine-based sorting pathway is required for CD4 down-regulation and optimal viral infectivity. Proc. Natl. Acad. Sci. USA *95*, 11229–11234.

Deacon, N.J., Tsykin, A., Solomon, A., Smith, K., Ludford-Menting, M., Hooker, D.J., McPhee, D.A., Greenway, A.L., Ellett, A., Chatfield, C., et al. (1995). Genomic structure of an attenuated quasi species of HIV-1 from a blood transfusion donor and recipients. Science *270*, 988–991.

Dong, X., Li, H., Derdowski, A., Ding, L., Burnett, A., Chen, X., Peters, T.R., Dermody, T.S., Woodruff, E., Wang, J.J., and Spearman, P. (2005). AP-3 directs the intracellular trafficking of HIV-1 Gag and plays a key role in particle assembly. Cell *120*, 663–674.

Elliott, G., and O'Hare, P. (1997). Intercellular trafficking and protein delivery by a herpesvirus structural protein. Cell *88*, 223–233.

Fackler, O.T., and Baur, A.S. (2002). Live and let die: Nef functions beyond HIV replication. Immunity *16*, 493–497.

Fackler, O.T., Luo, W., Geyer, M., Alberts, A.S., and Peterlin, B.M. (1999). Activation of Vav by Nef induces cytoskeletal rearrangements and downstream effector functions. Mol. Cell *3*, 729–739.

Fais, S., Capobianchi, M.R., Abbate, I., Castilletti, C., Gentile, M., Cordiali Fei, P., Ameglio, F., and Dianzani, F. (1995). Unidirectional budding of HIV-1 at the site of cell-to-cell contact is associated with co-polarization of intercellular adhesion molecules and HIV-1 viral matrix protein. AIDS *9*, 329–335.

Fomina, A.F., Deerinck, T.J., Ellisman, M.H., and Cahalan, M.D. (2003). Regulation of membrane trafficking and subcellular organization of endocytic

compartments revealed with FM1-43 in resting and activated human T cells. Exp. Cell Res. *291*, 150–166.

Garcia, J.V., and Miller, A.D. (1991). Serine phosphorylation-independent downregulation of cell-surface CD4 by nef. Nature *350*, 508–511.

Geisler, C. (2004). TCR trafficking in resting and stimulated T cells. Crit. Rev. Immunol. *24*, 67–86.

Geuskens, M., Torres, J.M., Esteban, C., and Uriel, J. (1989). Morphological characterization of the pathway of endocytosis and intracellular processing of transferrin and alpha-fetoprotein in human T lymphocytes stimulated with phytohemagglutinin (PHA). Eur. J. Cell Biol. *50*, 418–427.

Greenberg, M.E., Bronson, S., Lock, M., Neumann, M., Pavlakis, G.N., and Skowronski, J. (1997). Co-localization of HIV-1 Nef with the AP-2 adaptor protein complex correlates with Nef-induced CD4 down-regulation. EMBO J. *16*, 6964–6976.

Gundelfinger, E.D., Kessels, M.M., and Qualmann, B. (2003). Temporal and spatial coordination of exocytosis and endocytosis. Nat. Rev. Mol. Cell Biol. *4*, 127–139.

Haase, A.T. (2005). Perils at mucosal front lines for HIV and SIV and their hosts. Nat. Rev. Immunol. *5*, 783–792.

Hanna, Z., Kay, D.G., Rebai, N., Guimond, A., Jothy, S., and Jolicoeur, P. (1998). Nef harbors a major determinant of pathogenicity for an AIDS-like disease induced by HIV-1 in transgenic mice. Cell *95*, 163–175.

Hanna, Z., Priceputu, E., Hu, C., Vincent, P., and Jolicoeur, P. (2006). HIV-1 Nef mutations abrogating downregulation of CD4 affect other Nef functions and show reduced pathogenicity in transgenic mice. Virology *346*, 40–52.

Huang, J.F., Yang, Y., Sepulveda, H., Shi, W., Hwang, I., Peterson, P.A., Jackson, M.R., Sprent, J., and Cai, Z. (1999). TCR-Mediated internalization of peptide-MHC complexes acquired by T cells. Science *286*, 952–954.

Iafrate, A.J., Carl, S., Bronson, S., Stahl-Hennig, C., Swigut, T., Skowronski, J., and Kirchhoff, F. (2000). Disrupting surfaces of nef required for downregulation of CD4 and for enhancement of virion infectivity attenuates simian immunodeficiency virus replication in vivo. J. Virol. *74*, 9836–9844.

Igakura, T., Stinchcombe, J.C., Goon, P.K., Taylor, G.P., Weber, J.N., Griffiths, G.M., Tanaka, Y., Osame, M., and Bangham, C.R. (2003). Spread of HTLV-I between lymphocytes by virus-induced polarization of the cytoskeleton. Science *299*, 1713–1716.

Johnson, D.C., and Huber, M.T. (2002). Directed egress of animal viruses promotes cell-to-cell spread. J. Virol. *76*, 1–8.

Jolly, C., and Sattentau, Q.J. (2007). Regulated secretion from CD4+ T cells. Trends Immunol. *28*, 474–481.

Joly, E., and Hudrisier, D. (2003). What is trogocytosis and what is its purpose? Nat. Immunol. *4*, 815.

Kestler, H.W., 3rd, Ringler, D.J., Mori, K., Panicali, D.L., Sehgal, P.K., Daniel, M.D., and Desrosiers, R.C. (1991). Importance of the nef gene for maintenance of high virus loads and for development of AIDS. Cell *65*, 651–662.

Lama, J. (2003). The physiological relevance of CD4 receptor down-modulation during HIV infection. Curr. HIV Res. *1*, 167–184.

Lamparski, H.G., Metha-Damani, A., Yao, J.Y., Patel, S., Hsu, D.H., Ruegg, C., and Le Pecq, J.B. (2002). Production and characterization of clinical grade exosomes derived from dendritic cells. J. Immunol. Methods *270*, 211–226.

Le Gall, S., Erdtmann, L., Benichou, S., Berlioz-Torrent, C., Liu, L., Benarous, R., Heard, J.M., and Schwartz, O. (1998). Nef interacts with the mu subunit of clathrin adaptor complexes and reveals a cryptic sorting signal in MHC I molecules. Immunity *8*, 483–495.

Learmont, J.C., Geczy, A.F., Mills, J., Ashton, L.J., Raynes-Greenow, C.H., Garsia, R.J., Dyer, W.B., McIntyre, L., Oelrichs, R.B., Rhodes, D.I., et al. (1999). Immunologic and virologic status after 14 to 18 years of infection with an attenuated strain of HIV-1. A report from the Sydney Blood Bank Cohort. N. Engl. J. Med. *340*, 1715–1722.

Lindemann, D., Wilhelm, R., Renard, P., Althage, A., Zinkernagel, R., and Mous, J. (1994). Severe immunodeficiency associated with a human immunodeficiency virus 1 NEF/3′-long terminal repeat transgene. J. Exp. Med. *179*, 797–807.

Lu, X., Wu, X., Plemenitas, A., Yu, H., Sawai, E.T., Abo, A., and Peterlin, B.M. (1996). CDC42 and Rac1 are implicated in the activation of the Nef-associated kinase and replication of HIV-1. Curr. Biol. *6*, 1677–1684.

Madrid, R., Janvier, K., Hitchin, D., Day, J., Coleman, S., Noviello, C., Bouchet, J., Benmerah, A., Guatelli, J., and Benichou, S. (2005). Nef-induced alteration of the early/recycling endosomal compartment correlates with enhancement of HIV-1 infectivity. J. Biol. Chem. *280*, 5032–5044.

Martínez-Lorenzo, M.J., Anel, A., Gamen, S., Monleón, I., Lasierra, P., Larrad, L., Piñeiro, A., Alava, M.A., and Naval, J. (1999). Activated human T cells release bioactive Fas ligand and APO2 ligand in microvesicles. J. Immunol. *163*, 1274–1281.

Michel, N., Allespach, I., Venzke, S., Fackler, O.T., and Keppler, O.T. (2005). The Nef protein of human immunodeficiency virus establishes superinfection immunity by a dual strategy to downregulate cell-surface CCR5 and CD4. Curr. Biol. *15*, 714–723.

Monleón, I., Martínez-Lorenzo, M.J., Monteagudo, L., Lasierra, P., Taules, M., Iturralde, M., Piñeiro, A., Larrad, L., Alava, M.A., Naval, J., and Anel, A. (2001). Differential secretion of Fas ligand- or APO2 ligand/TNF-related apoptosis-inducing ligand-carrying microvesicles during activation-induced death of human T cells. J. Immunol. *167*, 6736–6744.

Morris, C.E., and Homann, U. (2001). Cell surface area regulation and membrane tension. J. Membr. Biol. *179*, 79–102.

Ono, A., and Freed, E.O. (2001). Plasma membrane rafts play a critical role in HIV-1 assembly and release. Proc. Natl. Acad. Sci. USA *98*, 13925–13930.

Pearce-Pratt, R., Malamud, D., and Phillips, D.M. (1994). Role of the cytoskeleton in cell-to-cell transmission of human immunodeficiency virus. J. Virol. *68*, 2898–2905.

Pelchen-Matthews, A., Kramer, B., and Marsh, M. (2003). Infectious HIV-1 assembles in late endosomes in primary macrophages. J. Cell Biol. *162*, 443–455.

Piguet, V., Chen, Y.L., Mangasarian, A., Foti, M., Carpentier, J.L., and Trono, D. (1998). Mechanism of Nef-induced CD4 endocytosis: Nef connects CD4 with the mu chain of adaptor complexes. EMBO J. *17*, 2472–2481.

Piguet, V., Schwartz, O., Le Gall, S., and Trono, D. (1999). The downregulation of CD4 and MHC-I by primate lentiviruses: a paradigm for the modulation of cell surface receptors. Immunol. Rev. *168*, 51–63.

Puente, L.G., He, J.S., and Ostergaard, H.L. (2006). A novel PKC regulates ERK activation and degranulation of cytotoxic T lymphocytes: Plasticity in PKC regulation of ERK. Eur. J. Immunol. *36*, 1009–1018.

Qiao, X., He, B., Chiu, A., Knowles, D.M., Chadburn, A., and Cerutti, A. (2006). Human immunodeficiency virus 1 Nef suppresses CD40-dependent immunoglobulin class switching in bystander B cells. Nat. Immunol. *7*, 302–310.

Raposo, G., Nijman, H.W., Stoorvogel, W., Liejendekker, R., Harding, C.V., Melief, C.J., and Geuze, H.J. (1996). B lymphocytes secrete antigen-presenting vesicles. J. Exp. Med. *183*, 1161–1172.

Rhee, S.S., and Marsh, J.W. (1994). Human immunodeficiency virus type 1 Nef-induced down-modulation of CD4 is due to rapid internalization and degradation of surface CD4. J. Virol. *68*, 5156–5163.

Robertson, L.K., Mireau, L.R., and Ostergaard, H.L. (2005). A role for phosphatidylinositol 3-kinase in TCR-stimulated ERK activation leading to paxillin phosphorylation and CTL degranulation. J. Immunol. *175*, 8138–8145.

Saag, M.S., Holodniy, M., Kuritzkes, D.R., O'Brien, W.A., Coombs, R., Poscher, M.E., Jacobsen, D.M., Shaw, G.M., Richman, D.D., and Volberding, P.A. (1996). HIV viral load markers in clinical practice. Nat. Med. *2*, 625–629.

Sandrin, V., and Cosset, F.L. (2006). Intracellular versus cell surface assembly of retroviral pseudotypes is determined by the cellular localization of the viral glycoprotein, its capacity to interact with Gag, and the expression of the Nef protein. J. Biol. Chem. *281*, 528–542.

Savina, A., Vidal, M., and Colombo, M.I. (2002). The exosome pathway in K562 cells is regulated by Rab11. J. Cell Sci. *115*, 2505–2515.

Schaefer, T.M., Bell, I., Fallert, B.A., and Reinhart, T.A. (2000). The T-cell receptor zeta chain contains two homologous domains with which simian immunodeficiency virus Nef interacts and mediates down-modulation. J. Virol. *74*, 3273–3283.

Schaft, N., Dörrie, J., Muller, I., Beck, V., Baumann, S., Schunder, T., Kämpgen, E., and Schuler, G. (2005). A new way to generate cytolytic tumor-specific T cells: electroporation of RNA coding for a T cell receptor into T lymphocytes. Cancer Immunol. Immunother. *55*, 1–10.

Schiavoni, I., Trapp, S., Santarcangelo, A.C., Piacentini, V., Pugliese, K., Baur, A., and Federico, M. (2004). HIV-1 Nef enhances both membrane expression and virion incorporation of Env products. A model for the Nef-dependent increase of HIV-1 infectivity. J. Biol. Chem. *279*, 22996–23006.

Seachrist, J.L., and Ferguson, S.S. (2003). Regulation of G protein-coupled receptor endocytosis and trafficking by Rab GTPases. Life Sci. *74*, 225–235.

Silvestri, G., Sodora, D.L., Koup, R.A., Paiardini, M., O'Neil, S.P., McClure, H.M., Staprans, S.I., and Feinberg, M.B. (2003). Nonpathogenic SIV infection of sooty mangabeys is characterized by limited bystander immunopathology despite chronic high-level viremia. Immunity *18*, 441–452.

Simmons, A., Aluvihare, V., and McMichael, A. (2001). Nef triggers a transcriptional program in T cells imitating single-signal T cell activation and inducing HIV virulence mediators. Immunity *14*, 763–777.

Sowinski, S., Jolly, C., Berninghausen, O., Purbhoo, M.A., Chauveau, A., Kohler, K., Oddos, S., Eissmann, P., Brodsky, F.M., Hopkins, C., et al. (2008). Membrane nanotubes physically connect T cells over long distances presenting a novel route for HIV-1 transmission. Nat. Cell Biol. *10*, 211–219.

Stoddart, C.A., Geleziunas, R., Ferrell, S., Linquist-Stepps, V., Moreno, M.E., Bare, C., Xu, W., Yonemoto, W., Bresnahan, P.A., McCune, J.M., and Greene, W.C. (2003). Human immunodeficiency virus type 1 Nef-mediated downregulation of CD4 correlates with Nef enhancement of viral pathogenesis. J. Virol. *77*, 2124–2133.

Stove, V., Van de Walle, I., Naessens, E., Coene, E., Stove, C., Plum, J., and Verhasselt, B. (2005). Human immunodeficiency virus Nef induces rapid internalization of the T-cell coreceptor CD8alphabeta. J. Virol. *79*, 11422–11433.

Stumptner-Cuvelette, P., Morchoisne, S., Dugast, M., Le Gall, S., Raposo, G., Schwartz, O., and Benaroch, P. (2001). HIV-1 Nef impairs MHC class II antigen presentation and surface expression. Proc. Natl. Acad. Sci. USA *98*, 12144–12149.

Swigut, T., Shohdy, N., and Skowronski, J. (2001). Mechanism for down-regulation of CD28 by Nef. EMBO J. *20*, 1593–1604.

Théry, C., Zitvogel, L., and Amigorena, S. (2002). Exosomes: composition, biogenesis and function. Nat. Rev. Immunol. *2*, 569–579.

Wei, B.L., Arora, V.K., Foster, J.L., Sodora, D.L., and Garcia, J.V. (2003). In vivo analysis of Nef function. Curr. HIV Res. *1*, 41–50.

Williams, G.S., Collinson, L.M., Brzostek, J., Eissmann, P., Almeida, C.R., McCann, F.E., Burshtyn, D., and Davis, D.M. (2007). Membranous structures transfer cell surface proteins across NK cell immune synapses. Traffic *8*, 1190–1204.

Witte, V., Laffert, B., Rosorius, O., Lischka, P., Blume, K., Galler, G., Stilper, A., Willbold, D., D'Aloja, P., Sixt, M., et al. (2004). HIV-1 Nef mimics an integrin receptor signal that recruits the polycomb group protein Eed to the plasma membrane. Mol. Cell *13*, 179–190.

Witte, V., Laffert, B., Gintschel, P., Krautkramer, E., Blume, K., Fackler, O.T., and Baur, A.S. (2008). Induction of HIV transcription by Nef involves Lck activation and protein kinase C theta raft recruitment leading to activation of ERK1/2 but not NF kappa B. J. Immunol. *181*, 8425–8432.

Wolf, D., Giese, S.I., Witte, V., Krautkrämer, E., Trapp, S., Sass, G., Haller, C., Blume, K., Fackler, O.T., and Baur, A.S. (2008a). Novel (n)PKC kinases phosphorylate Nef for increased HIV transcription, replication and perinuclear targeting. Virology *370*, 45–54.

Wolf, D., Witte, V., Clark, P., Blume, K., Lichtenheld, M.G., and Baur, A.S. (2008b). HIV Nef enhances Tat-mediated viral transcription through a hnRNP-K-nucleated signaling complex. Cell Host Microbe *4*, 398–408.

Xu, X.N., Screaton, G.R., Gotch, F.M., Dong, T., Tan, R., Almond, N., Walker, B., Stebbings, R., Kent, K., Nagata, S., et al. (1997). Evasion of cytotoxic T lymphocyte (CTL) responses by nef-dependent induction of Fas ligand (CD95L) expression on simian immunodeficiency virus-infected cells. J. Exp. Med. *186*, 7–16.